A (U)MP2(full) and (U)CCSD(T) theoretical investigation into the substituent effects on the intermolecular T-shaped F–H…π interactions between HF and LBBL (L = −H, : CO, :NN, –Cl, –CN and –NC)

Zhao-ming Yang · Lin Zhang · Li-zhen Chen · Fu-de Ren · Shan Du · Lei Yang

Abstract The substituent effects on the intermolecular T-shaped F–H…π interactions are investigated between HF and LBBL (L = −H, : CO, :NN, –Cl, –CN and –NC) using the (U)MP2(full) and (U)CCSD(T) methods with the 6-311++G(2 d,p) basis set. The B ≡ B triple-bond contraction is found in the complexes with lone-pair-electron donors while the B = B double-bond is lengthened in the systems with the single-electron substituents upon complexation. The T-shaped F–H…π interaction energies follow the order of ClB = BCl… HF>HB = BH…HF>NNB ≡ BNN…HF>OCB ≡ BCO… HF>CNB = BNC…HF>NCB = BCN…HF. The electron-donating substituents : CO and :NN increases electron density of the B ≡ B triple bond by the delocalization interaction $E^{(2)}\pi_{(CO/NN)\rightarrow Lp(B)}$ while the electron-withdrawing substituents –CN and –NC decrease electron density of the B = B double bond by means of the π-π conjugative effect. The analyses of the APT atomic

charge, "truncated" model, natural bond orbital (NBO), atoms in molecules (AIM) and electron density shifts reveal the nature of the substituent effect and explain the origin of the B ≡ B bond contraction.

Introduction

Recently substituent effects on T-shaped X–H…π interactions have received much attention in experimental and theoretical investigations as a result of their extremely important role in determining the structures and activities of organic, organometallic and biological molecules [1]. Ehama et al. have found that the T-shaped C–H…π interaction between chloroform and arene becomes stronger when the arene becomes more electron-rich [2]. The contribution of the charge-transfer term to the T-shaped C–H…π interaction has been supported by ab initio calculations and experiments on the substituent effect [3, 4]. In 2004, a theoretical study of the intramolecular C–H…π interaction showed that the electron-donor or electron-withdrawing character had an important influence on the population of the T-shaped C–H…π bond [5]. In 2006, Vaupel et al. investigated the characterization of the T-shaped N–H…π intermolecular interactions of ammonia with various substituted π-systems. They found that the polarizabilities of the π-electron systems mainly by the substituents played an important role in governing the nature and geometry of the N–H…π interaction [6]. In 2008, a theoretical

Z.-m. Yang · L.-z. Chen · F.-d. Ren (✉) · S. Du · L. Yang
College of Chemical Engineering and Environment,
North University of China,
Taiyuan 030051, China
e-mail: renfude@hotmail.com

F.-d. Ren
e-mail: fdren888@126.com

L. Zhang
Department of Chemistry, College of Science,
North University of China,
Taiyuan 030051, China

(B3LYP/6-31 G**) and experimental study on the strength of the T-shaped N–H…π hydrogen bonds based on the tautomeric equilibria of 30 substituted NH-pyrazoles was carried out. The result showed that the strength of the N–H…π hydrogen bond depended on the electronic effect of the substituent [7]. Subsequently, systematic trends in the pyrrole dimer N–H…π interaction as a function of methyl substitution were identified [8]. Furthermore, the substituent effect on the T-shaped O–H…π interaction was also investigated using high-resolution UV spectroscopy and ab initio calculations [9]. All the previous investigations paid close attention to substituent effects on the T-shaped X–H…π interactions containing only the substituted electron-rich aromatic ring or CC multiple-bond. However, to our knowledge, no study on substituent effect on the T-shaped X–H…π interactions involving the electron-deficient multiple bond has been presented.

The BB bond is the typical electron-deficient multiple-bond [10]. Recently we have found that the investigation on the monomer and T-shaped X–H…π hydrogen-bonded complex involving the BB multiple-bond has always been of the interesting topic, accompanied by the unusual "phenomenon" [11–13]. For example, the electron-deficient BB bond in LBBL shows the double-bond and triple-bond characteristic with the single-electron donating/withdrawing (L = −H, –CN, –F, etc.) and lone-pair-electron donating (L = : CO, :NN, etc.) substituent, respectively [11, 12, 14], as is just opposite to the electron-rich CC bond in LCCL [15–19]. Knight and Jouany et al. have found the valence molecular orbitals of HBBH were $(2\sigma_g)^2 (2\sigma_u)^2 (3\sigma_g)^2 (1\pi_u)^2$ where the two paired electrons occupied degenerate boron 2p bonding orbitals, indicating that HBBH contained one B–B π bonding orbital [10, 11]. Papakondylis et al. examined the OCBBCO and NNBBNN molecules using the coupled-cluster methodology and large correlation consistent basis sets. They found that the bonding mechanism of BCO or BN$_2$ was due to charge transfer from L to the empty $2p_z$ orbital of the B atom and the LBBL series resulted by singlet coupling two B–Y$^4 \sum^-$ moieties, leading to acetylene-like LBBL systems of the $^1\sum_g^+$ symmetry [12]. In the investigation on the T-shaped X–H…π hydrogen-bonded complexes involved with the B $\equiv$ B bond, we have found that the B $\equiv$ B triple bond underwent contraction [13], as is not consistent with the accepted notion that the multiple bond should be elongated as a result of H…π interaction [20–24]. Furthermore, we have drawn a conclusion that the lost densities from the C $\equiv$ O group are shifted to the π-bonding orbital of the B $\equiv$ B bond upon the formation of the T-shaped X–H…π interaction, leading to the electron density accumulation

in the B $\equiv$ B bond and the contraction of the B $\equiv$ B bond [13]. Moreover, we have also confirmed that, although the BB bond is electron-deficient, it can be the stronger T-shaped X–H…π hydrogen-bond proton acceptor than the CC multiple-bond [23].

As a follow-up to our investigations on the H…π hydrogen-bonded complexes involving the electron-deficient BB multiple-bond above, in this paper, our goal is mainly to discuss systematically the substituent effect on the intermolecular T-shaped F–H…π interaction between HF and LBBL with the single-electron substituents (L = −H, –F, –Cl, –CN and –NC) or lone-pair-electron groups (L = : CO and : NN). This theoretical investigation will reveal the nature of the substituent effect to further study on structure and activity for the T-shaped X–H…π hydrogen-bonded complex involving LBBL with the electron-donating or withdrawing substituent in theory and experiment.

Computational methods

It is well-established that, in most cases, the MP2(full) and CCSD(T) methods are reliable and have been applied successfully to investigate the intermolecular interactions [25, 26]. Furthermore, we have found that the 6-311++G(2 d,p) basis set can be applied to reveal the nature of the intermolecular T-shaped X–H…π interactions [13]. So we used the MP2(full) and CCSD(T) methods with the 6-311++G(2 d,p) basis set for monomers and F–H…LBBL in this paper. For the open-shell systems (L = −H, –F, –Cl, –CN and –NC), the UMP2(full) and UCCSD(T) methods were also employed.

All the calculations have been performed using Gaussian 03 programs [27]. All the possible T-shaped F–H…π hydrogen-bonded complexes have been fully optimized using the (U)B3LYP/6-311++G(2 d,p) and (U)MP2(full)/6-311++G(2 d,p) methods. The structures corresponding to the minimum energy points at the molecular energy hypersurface have been obtained. Single point energy calculations have been performed at (U)B3LYP/6-311++G(2 d,p), (U)MP2(full)/6-311++G(2 d,p) and (U)CCSD(T)/6-311++G(2 d,p) levels, respectively. The natural bonding analysis [28] has been carried out with (U)MP2(full)/6-311++G(2 d,p) method. The shifts of the electron densities [29] that accompany the formation of the T-shaped F–H…π interactions have been displayed at (U)MP2(full)/6-311++G(2 d,p) level using GaussView program and the topological electron charge density has been analyzed by the AIM method [30] using AIMPAC program [31] at the same level. The frequency shifts ($\Delta\nu$), defined as the difference between the frequency of the

certain vibrational mode in the complex and in the isolated monomer, can be expressed as follows:

$$\Delta v = v_{\text{complex}} - v_{\text{monomer}}. \tag{1}$$

Binding energy (D_e) is calculated from the expression:

$$D_e = E_{\text{(FH–LBBL)com.}} - E_{\text{(LBBL)mono.}} - E_{\text{(FH)mono.,}} \tag{2}$$

where $E_{\text{(FH–LBBL)com.}}$ is the energy of the complex. $E_{\text{(LBBL)mono.}}$ and $E_{\text{(FH)mono.}}$ are the energies of monomers. The D_e corrected for the basis set superposition error (BSSE) [32, 33] and zero-point energy (ZPE) correction has been evaluated.

Results and discussion

Our preliminary calculations indicate that the isolated triplet state monomer LBBL ($^3\Sigma_g^-$) (L = –H, –F, –Cl, –CN or –NC) is lower in energy than the corresponding singlet state LBBL ($^1\Delta_g$). However, the T-shaped F–H…π interactions between the triplet state LBBL and HF are weaker than those of the singlet state LBBL with HF, as is in accordance with our previous investigation [23]. Therefore, we present here only the theoretical study on the T-shaped F–H…π hydrogen-bonded complexes of the singlet state LBBL with HF. On the other hand, the T-shaped H…π hydrogen-bonded complex FBBF…HF (C_{2v}) is not a minimum energy point at the molecular energy hypersurface ("Convergence failure" in geometry optimization is shown at (U)B3LYP/6-311++G(2 d,p) or (U)MP2(full)/6-311++G(2 d,p) level). The local minimum or global minimum energy point of FBBF…HF (C_{2v}) is not found. Thus, only six complexes are obtained. The atomic labels and bond critical points (BCPs) of the complexes are shown in Fig. 1, and the corresponding geometries parameters and the electron densities at the BCPs are listed in Table 1. APT and natural charges as well as the binding energies are given in Tables 2 and 3, respectively. The frequency shifts and natural bond orbital (NBO) analysis are presented in Tables 4 and 5, respectively. The "truncated" model and shifts of electron densities are illustrated in Figs. 2 and 3, respectively.

Equilibrium geometry

The structures of the monomers LBBL are all $D_{\infty h}$ symmetry. The corresponding complexes form the C_{2v} T-shape with F–H lying perpendicular to the BB bond and pointing toward to its midpoint (see Fig. 1).

From Table 1, for the T-shaped F–H…π hydrogen-bonded complexes with the single-electron substituents –Cl, –CN and –NC, the distances of H…π bond are 2.153,

2.352 and 2.278 Å at (U)MP2(full)/6-311++G(2 d,p) level, respectively. The distance of H…π bond in ClB = BCl…HF is shorter than that in HB = BH…HF (2.217) while the distance of H…π bond in NCB = BCN…HF or CNB = BNC…HF is larger than that in HB = BH…HF. This result shows that the substituent –Cl might increase T-shaped F–H…π interaction compared with HB = BH…HF, while the H…π interaction in NCB = BCN…HF or CNB = BNC…HF might be weaker than that in HBBH…HF.

In the T-shaped F–H…π hydrogen-bonded complexes with the lone-pair-electron substituents : CO and :NN, the distances of H…π bond are 2.236 and 2.209 Å at (U)B3LYP/6-311++G(2 d,p) level, respectively. The distance of H…π bond in NNB ≡ BNN…HF or OCB ≡ BCO…HF is larger than that in HB = BH…HF (2.178 Å at (U)B3LYP/6-311++G(2 d,p) level). The reason might simply be that the substituent groups : CO and :NN are much lager than H. Thus, it is easy for HF to come closer to HBBH. At (U)MP2(full)/6-311++G(2 d,p) level, the distance of H…π bond in OCB ≡ BCO…HF (2.300 Å) is also found to be larger than that in HB = BH…HF. For the H…π hydrogen-bonded complex NNB ≡ BNN…HF (C_{2v}), "Convergence failure" in geometry optimization is shown at (U)MP2(full)/6-311++G(2 d,p) level, and the local minimum or global minimum energy point is not found using this method. These results suggest that the T-shaped F–H…π interaction in OCB ≡ BCO…HF or NNB ≡ BNN…HF might be weaker than that in HB = BH…HF. In our previous investigations, we have also found that the distance of H…π bond in OCB ≡ BCO…HF is larger than that in HB = BH ($^1\Delta_g$)…HF [23].

From Table 1, at (U)MP2(full)/6-311++G(2 d,p) and (U)B3LYP/6-311++G(2 d,p) levels, the F–H bond length in ClB = BCl…HF is larger than that in HB = BH…HF while the F–H bond length in the other complex is shorter than that in HB = BH…HF. This result also indicates that the H…π interaction in ClBBCl…HF might be stronger than that in HB = BH…HF while the H…π interaction in LBBL…HF (L = : CO, : NN, –CN or –NC) might be weaker than that in HB = BH…HF.

In general, in the T-shaped X–H…π interaction complex, the multiple-bond will be weakened and elongated due to electron transfer from the π-bonding orbital of the multiple-bond toward H–X upon complexation. For example, McDowell and Tavares et al. have found that, for the T-shaped X–H…π interaction complexes involving the CC multiple-bond, both the C = C and C ≡ C bonds are elongated in comparison with those in monomers [21, 34]. In our recent investigation on the T-shaped X–H…π hydrogen-bonded complex HB = BH($^1\Delta_g$)…HX, the B = B double bond was also elongated [22]. However, for the T-shaped X–H…π hydrogen-bonded complexes OCB ≡
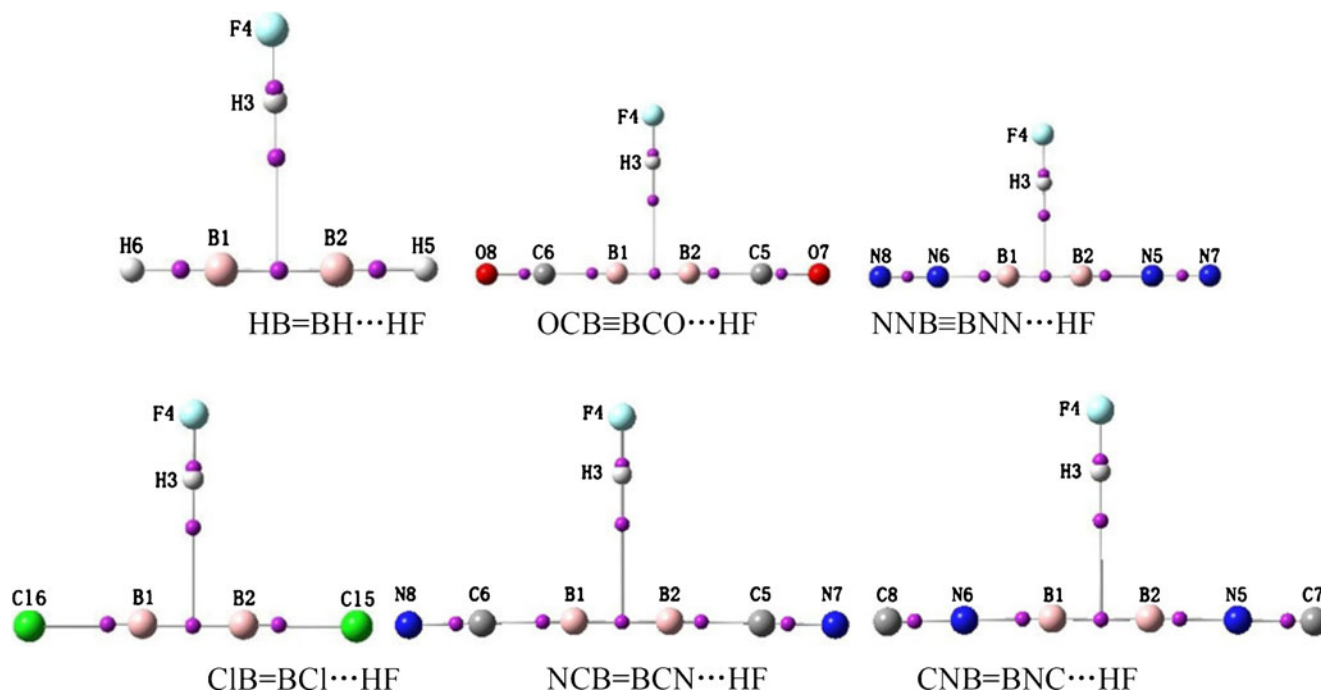
Fig. 1 Molecular structures and bond critical points of the complexes

BCO…HX, we have found that the B ≡ B triple bond undergoes contraction from 1.510 to 1.500, 1.503, 1.504 and 1.507 Å in OCB ≡ BCO…H–X (X = −F, –Cl, –CN and –C_2H) at MP2/6-311++G(2 d,p) level, respectively [13].

In this work, we have found the increment of the BB bond length in the complexes involving the B = B double-bond whereas the contraction in the complexes involved with the B ≡ B triple-bond. From Table 1, for OCB ≡ BCO…HF, the B ≡ B triple bond is contracted from 1.505 Å to 1.496 Å at (U)MP2(full)/6-311++G(2 d,p) level. In NNB ≡ BNN…HF, the B ≡ B triple bond is contracted from 1.436 Å to 1.432 Å at (U)B3LYP/6-311++G(2 d,p) level. However, in the HF complexes with LB = BL (L are the single-electron substituents –H, –Cl, –CN and –NC), the B = B double bonds are lengthened from 1.525, 1.505, 1.521 and 1.509 Å to 1.527, 1.508, 1.523 and 1.511 Å at (U)MP2(full)/6-311++G(2 d,p) level, respectively. Thus, we might conclude that the B ≡ B triple bond will be contracted in the complex with the lone-pair-electron donor substituent while the B = B double bond might be lengthened for the system with the single-electron substituent upon complexation.

As can be seen from Table 1, the distance of H…π is the order of ClB = BCl…HF<HB = BH…HF<OCB ≡ BCO…HF<CNB = BNC…HF<NCB = BCN…HF at (U)MP2(full)/6-311++G(2 d,p) level, whereas the order of the increment of the F–H bond length is ClB = BCl…HF>HB = BH…HF>CNB = BNC…HF>OCB ≡ BCO…HF>NCB = BCN…HF. These results suggest that the T-shaped F–H…π interactions might follow the order of

ClB = BCl…HF>HB = BH…HF>OCB ≡ BCO…HF>NCB = BCN…HF.

APT atomic charge

In most cases, the APT atomic charges are reliable to be applied to investigate the electron-donating/withdrawing ability of a group [35]. The APT charge of the BB bond (the sum of the APT atomic charges of two boron atoms) can be used to roughly represent electron-donating/withdrawing ability of the BB bond, thus, indicating indirectly the electron-donating/withdrawing ability of substituent, too.

From Table 2, the values of the APT charge of the BB bond in the monomers OCB ≡ BCO and NNB ≡ BNN are negative, indicating the electron-donating characteristic of the substituents : CO and : NN. It is noteworthy that, although the electronegativity of the C, O and N atoms is higher than that of the B atom, and the electrons should transfer from BB to : CO and : NN, the electrons shift conversely, perhaps due to that these substituents have lone-pair electrons and the boron atom is electron-deficient. Thus, the substituents might offer the lone-pair electrons to the electron-deficient boron atom, as is in accordance with the investigation by Papakondylis et al. [12].

For the monomers LBBL (L = −Cl, –CN and –NC) as well as their complexes, the values of the APT charges of the BB bond are positive, indicating that –Cl, –CN and –NC are the electron-withdrawing substituents in monomers and complexes.

Table 1 Principal geometry parameters (in Å) and selected bond critical point properties (in a.u., at (U)MP2(full)/6-311++G(2 d,p) level) for the monomers (in bold) and complexes[a]

Parameters	HBBH...HF	OCBBCO...HF	NNBBNN...HF[c]	ClBBCl...HF	NCBBCN...HF	CNBBNC...HF
$R(H{\cdots}\pi)$	2.217 (2.178)	2.300 (2.236)	(2.209)	2.153 (2.134)	2.352 (2.322)	2.278 (2.252)
$R(B{-}B)$	1.527 (1.522) 1.525 (1.520)	1.496 (1.441) 1.505 (1.444)	(1.432) (1.436)	1.508 (1.502) 1.505 (1.498)	1.523 (1.515) 1.521 (1.513)	1.511 (1.509) 1.509 (1.507)
$R(H{-}F)$[b]	0.939 (0.947)	0.929 (0.937)	(0.940)	0.942 (0.949)	0.930 (0.935)	0.933 (0.939)
$R(B{-}L)$	1.170 (1.169) 1.171 (1.170)	1.420 (1.440) 1.440 (1.434)	(1.376) (1.370)	1.680 (1.683) 1.688 (1.690)	1.470 (1.460) 1.470 (1.460)	1.373 (1.360) 1.375 (1.361)
$\rho_{BCP(H{\cdots}\pi)}$	0.0220	0.0152	(0.0192)	0.0250	0.0159	0.0193
$\nabla^2\rho_{BCP(H{\cdots}\pi)}$	0.0382	0.0350	(0.0354)	0.0415	0.0358	0.0380
$\rho_{BCP(B{-}B)}$	0.1973 0.1985	0.1871 0.1868	(0.2036) (0.2046)	0.1921 0.1930	0.1962 0.1972	0.1934 0.1945
$\nabla^2\rho_{BCP(B{-}B)}$	-0.5085 -0.5130	-0.3835 -0.4136	(-0.4335) (-0.4537)	-0.3884 -0.3832	-0.4924 -0.4961	-0.4411 -0.4395
$\rho_{BCP(H{-}F)}$[d]	0.3380	0.3520	(0.3459)	0.3351	0.3526	0.3471
$\nabla^2\rho_{BCP(H{-}F)}$	-2.7334	-2.8988	(-2.5379)	-2.6759	-2.8593	-2.8199
$\rho_{BCP(B{-}L)}$	0.1974 0.1953	0.1989 0.2010	(0.1966) (0.1992)	0.1717 0.1681	0.2041 0.2030	0.2150 0.2133
$\nabla^2\rho_{BCP(B{-}L)}$	-0.3861 -0.3640	0.4607 0.4676	(0.7864) (0.7985)	0.0295 0.0403	-0.0145 -0.0004	0.6594 0.6647

[a] The values out of the parenthesis are obtained at (U)MP2(full)/6-311++G(2 d,p) level, while those in the parenthesis are from the (U)B3LYP/6-311++G(2 d,p) method

[b] In the isolated monomer, the H–F bond length is 0.924 Å at (U)B3LYP/6-311++G(2 d,p) level, and 0.922 Å at (U)MP2(full)/6-311++G(2 d,p) level

[c] For NNBBNN and NNBBNN...HF, geometry parameter and bond critical point property are obtained at (U)B3LYP/6-311++G(2 d,p) level

[d] In the isolated monomer, the value of $\rho_{BCP(H{-}F)}$ is 0.3652 and that of $\nabla^2\rho_{BCP(H{-}F)}$ is -2.9717 at (U)MP2(full)/6-311++G(2 d,p) level

Table 2 APT charges (in plain, in e, at (U)B3LYP/6-311++G(2 d,p) level) and natural charges (in bold, in e, at (U)MP2(full)/6-311++G(2 d,p) level) for the complexes and the monomers (in parentheses)

Parameters	HBBH...HF	OCBBCO...HF	NNBBNN...HF[a]	ClBBCl...HF	NCBBCN...HF	CNBBNC...HF
Q_{B-B}	0.142 (0.066) 0.256 (0.234)	-0.912 (-0.926) -0.560 (-0.484)	-0.722 (-0.724) 0.068 (0.148)	0.732 (0.682) 0.284 (0.290)	0.540 (0.474) 0.620 (0.640)	0.792 (0.696) 0.934 (0.942)
Q_{H3}	0.541 0.565	0.427 0.580	0.445 0.554	0.525 0.569	0.439 0.565	0.470 0.565
Q_{F4}	-0.631 -0.615	-0.502 -0.591	-0.517 -0.577	-0.622 -0.613	-0.506 -0.582	-0.547 -0.596
$Q_{L5/L6}$	-0.025 (-0.330) -0.103 (-0.117)	1.428 (1.436) 0.752 (0.730)	1.077 (1.109) -0.130 (-0.141)	-0.315 (-0.341) -0.116 (-0.145)	-0.047 (0.028) -0.119 (-0.107)	-0.552 (-0.446) -0.978 (-0.965)
$Q_{X7/X8}$		-0.926 (-0.973) -0.466 (-0.488)	-0.680 (-0.747) 0.107 (0.068)		-0.190 (-0.264) -0.184 (-0.212)	0.194 (0.980) 0.525 (0.494)

[a] For NNBBNN and NNBBNN...HF, APT charge and natural charge are obtained at (U)B3LYP/6-311++G(2 d,p) level

Table 3 Binding energies of complexes ($-D_e$ (kJ mol^{-1}))

Parameters	HBBH...HF	OCBBCO...HF	NNBBNN...HF[a]	ClBBCl...HF	NCBBCN...HF	CNBBNC...HF
(U)B3LYP/6-311++G(2 d,p)	31.11 30.06 [a] 25.89 [b]	16.42 14.90 10.10 5.95 27.01 33.00 [c]	17.67 16.07 11.74 5.95 20.36 26.31 [c]	31.20 30.13 25.28 −15.32 32.61 0.21 17.08 [d]	8.64 7.17 4.58 −23.40 31.48 0.37 7.71 [d]	14.52 7.93 5.46 −20.22 30.06 0.15 9.69 [d]
(U)MP2(full)/6-311++G(2 d,p)	28.97 24.94 20.41	15.41 11.27 9.22	16.79 14.28 7.10 2.39 9.49	30.60 25.23 20.77 −12.59 29.82 1.37 15.86	10.52 6.75 5.15 −21.17 29.00 1.57 6.26	14.75 10.74 8.44 −17.13 28.17 1.63 9.41
(U)CCSD(T)/6-311++G(2 d,p)	24.69 20.96	18.98 15.22	6.62 26.13 32.75	27.18 22.30 −11.97 26.13 1.59 12.57	8.20 4.69	13.52 9.80 −17.05 24.49 1.80 5.64

[a] The binding energies in italic are BSSE correct energies

[b] The binding energy with BSSE and ZPE ($-D_{e(\text{BSSE-ZPE})}$) correction

[c] The binding energies in bold are obtained by "truncated" model. They are $-E_{\text{int}(L...HF...L)}$, $-E_{\text{int}(FH...BB)}$, and $-[E_{\text{int}(L...HF...L)} + E_{\text{int}(FH...BB)}]$, respectively

[d] The binding energies in bold are obtained by "truncated" model. They are $-E_{\text{int}(LH...HF...HL)}$, $-E_{\text{int}(FH...HBBH)}$, $-E_{\text{int}(FH...HBBH)} + E_{\text{int}(LH...HF...HL)} + E_{\text{int}(H2...HF...H2)}$ and $-[E_{\text{int}(LH...HF...HL)} + E_{\text{int}(H2...HF...H2)}]$, respectively

As can be seen from Table 2, the order of the APT charge of the BB bond is as follows: OCB ≡ BCO < NNB ≡ BNN and NCB = BCN < ClB = BCl < CNB = BNC. This result shows that the order of the electron-donating ability of substituent might be OCB ≡ BCO > NNB ≡ BNN, and that of the electron-withdrawing ability might be NCB = BCN < ClB = BCl < CNB = BNC.

Binding energies and stabilities

Table 3 gives both uncorrected and corrected binding energies after correction of the ZPE and BSSE by means of the counterpoise method. From Table 3, the proportions of corrected interaction energies to their total binding energies, defined as $[(-D_e)-(-D_{e(\text{BSSE/ZPE})})]/(-D_e)$, are up to 45.31%, 35.71% and 42.68% at (U)B3LYP/6-311++G (2 d,p), (U)MP2(full)/6-311++G(2 d,p) and (U)CCSD(T)/6-311++G(2 d,p) levels for BSSE corrections, respectively. These results indicate that it is necessary for the T-shaped F–H...π interaction energies to check the BSSE corrections using these three methods, as is in accordance with our recent studies [26, 35]. In fact, there is a standard computational protocol, which requires BSSE corrections for intermolecular interaction energies. Only in the case of a complete basis set, the correction for BSSE is not needed. The ZPE corrections for the (U)B3LYP/6-311++G(2 d,p) and (U)MP2(full)/6-311++G(2 d,p) methods, which amount to 29.98 % and 37.69 %, respectively, might not be negligible, too. Our previous investigations have shown that the ZPE corrections for the T-shaped X–H...π interactions between HB=BH ($^1\Delta_g$) and HX are up to 74.40 % and 77.05 % at the B3LYP/6-311++G(2df,2p) and MP2/6-311++G(2df,2p) levels [22], and those for the H...π interactions between OCB ≡ BCO and HX are up to 47.53 % and 40.28 %, respectively [13].

As can be seen from Table 3, the T-shaped F–H...π interaction energies are in the order of ClB = BCl... HF>HB = BH...HF>NNB ≡ BNN...HF>OCB ≡ BCO... HF>CNB = BNC...HF>NCB = BCN...HF, which is in good agreement with the analysis of the H...π distance. Obviously, the lone-pair-electron substituents : NN and : CO decrease the T-shaped F–H...π interaction (in comparison with that of HB = BH($^1\Delta_g$)...HF). In our previous investigation, we also found that the T-shaped F–H...π interaction in OCBBCO...HF was weaker than that in HBBH ($^1\Delta_g$)...HF [23]. In the recent investigation on the cation-π interaction, we have confirmed that, although : CO is the electron-donating substituent, the cation-π interaction in OCBBCO...Na$^+$ is weaker than that in HBBH ($^1\Delta_g$)...Na$^+$, too [25]. It is worth mentioning that, our preliminary calculations indicate that the H...π interaction in OCBBCO...HF or NNBBNN...HF is far stronger than that in HBBH ($^3\Sigma_g^-$)...HF. For the

Table 4 Selected frequency shifts relative to the monomers for the complexes at (U)MP2(full)/6-311++G(2 d,p) level[a]

	HBBH…HF	OCBBCO…HF	NNBBNN…HF [c]	ClBBCl…HF	NCBBCN…HF	CNBBNC…HF
	$\Delta\nu/\nu_{com}I_{com}(I_{mono})$	$\Delta\nu/\nu_{com}I_{com}(I_{mono})$	$\Delta\nu/\nu_{com}I_{com}(I_{mono})$	$\Delta\nu/\nu_{com}I_{com}(I_{mono})$	$\Delta\nu/\nu_{com}I_{com}(I_{mono})$	$\Delta\nu/\nu_{com}I_{com}(I_{mono})$
ν_1	150, 0	125, 0	147, 1	225, 7	131, 3	141, 2
ν_2[b]	−401, 1177	−165, 561	−342, 903	−472, 1235	−206, 697	−273, 854
ν_3	−2, 0 (0)	13, 1 (0)	−27, (0)	−4, 2 (0)	1, 0 (0)	1, 0 (0)
ν_4		18, 5 (0)	23, 8 (0)		8, 0 (0)	16, 0 (75)
ν_5		15, 2536 (2623)	25,1801(2011)		6, 101 (47)	7, 573 (295)
ν_6	9, 9 (20)	−4, 20 (6)	12,102 (92)	16, 329 (303)	5, 50 (35)	7, 120 (94)

[a] All frequencies (ν or $\Delta\nu$) are in cm^{-1} and IR intensities (I) are in km mol^{-1}. ν_1, ν_2, ν_3, ν_4, ν_5 and ν_6 stand for stretching of H$^+$…π, stretching of HF, stretching of B–B, symmetrical stretching of L5–X7, anti-symmetrical stretching of L5–X7 and anti-symmetrical stretching of B–L5, respectively

[b] The frequencies of the isolated HF monomers is 4133 cm^{-1}, and the corresponding IR intensity is 138 km mol^{-1}

[c] For NNBBNN…HF, frequency shifts are obtained at (U)B3LYP/6-311++G(2 d,p) level

complex with electron-withdrawing substituent –CN or –NC, the interaction energy decreases compared with that of HB = BH…HF. However, although –Cl is also an electron-withdrawing substituent, the T-shaped F–H…π interaction energy in ClB = BCl…HF is stronger than that in HB = BH…HF. Again, it should be noted that the distance of H…π in ClB = BCl…HF is shorter than that in HB = BH…HF while the F–H bond length

in ClB = BCl…HF is larger than that in HB = BH…HF (see Table 1).

The calculated binding energy difference [$D_{e\ (LBBL…HF)}$−$(D_{e\ (HBBH…HF)})$] between LBBL…HF and HBBH…HF is as follows: –5.71 kJ mol^{-1} (23.13%), 2.49 kJ mol^{-1} (10.09%), –16.49 kJ mol^{-1} (66.79%) and –11.17 kJ mol^{-1} (45.24%) for the complexes with the substituents L = : CO, –Cl, –CN and –NC at (U)CCSD(T)/6-311++G(2 d,p) level,

Table 5 Calculated parameters of complexes at their equilibrium geometries: NBO occupation numbers for the BB and LX bonds or the B and Cl atoms with lone pairs (Occ.(BB) and Occ.(LX) or Occ.(B) and Occ.(Cl)), the (HF)*, (LX)* and (BB)* antibonds (Occ.(HF)*, Occ.(LX)* and Occ.(BB)*), their second-order perturbation energies $E^{(2)}$ and the NBO charge transfers of the monomers LBBL in their complexes (Q) at (U)MP2(full)/6-311++G(2 d,p) level

Parameters	HBBH…HF	OCBBCO…HF	NNBBNN…HF [f]	ClBBCl…HF	NCBBCN…HF	CNBBNC…HF
Occ.(BB) [a]	1.9467 p$^{1.00}$p$^{1.00}$	1.9717 sp$^{0.63}$sp$^{0.63}$	1.9677 sp$^{0.54}$sp$^{0.54}$	1.9417 p$^{1.00}$p$^{1.00}$	1.8420 p$^{1.00}$p$^{1.00}$	1.8461 p$^{1.00}$p$^{1.00}$
Occ.(HF)*	0.0498 sp$^{2.78}$	0.0136 sp$^{3.04}$	0.0291 sp3.24	0.0443 sp$^{2.78}$	0.0182 sp$^{3.16}$	0.0310 sp$^{3.00}$
$E^{(2)}\pi_{(BB)\to\sigma_{(HF)*}}$ [b]	98.32	3.51 [e]	6.77 [g]	85.52	39.14	57.84
Occ.(LX) [c]		1.9907 p$^{1.00}$p$^{1.00}$	1.9729 p$^{1.00}$p$^{1.00}$			
Occ.(LX)*					0.0690 p$^{1.00}$p$^{1.00}$	0.0575 p$^{1.00}$p$^{1.00}$
$E^{(2)}\pi_{(BB)\to\pi_{(LX)*}}$					115.93	85.90
Occ.(BB)*				0.1123 p$^{1.00}$p$^{1.00}$		
Occ.(B)		0.7973 p$^{1.00}$	0.7424 p$^{1.00}$			
$E^{(2)}\pi_{(LX)\to Lp(B)}$		21.12	40.40			
Occ.(Cl)				1.9376 p$^{1.00}$		
$E^{(2)}_{Lp(Cl)\to\pi_{(BB)*}}$				105.85		
$Q_{(LBBL)}$ [d]	50.23	10.55	22.96	44.00	16.88	30.89

[a] Occ.: occupation number

[b] In kJ mol^{-1}

[c] X means the O, N, N and C atoms at OCBBCO…HF, NNBBNN…HF, NCBBCN…HF and CNBBNC… HF, respectively

[d] In me

[e] Another notable stabilization energy $E^{(2)}_{Lp(B)\to\sigma(HF)*}$ is found to be 11.54 kJ mol^{-1}

[f] At (U)B3YP/6-311++G(2 d,p) level

[g] Another notable stabilization energy $E^{(2)}_{Lp(B)\to\sigma(HF)*}$ is found to be 13.42 kJ mol^{-1}
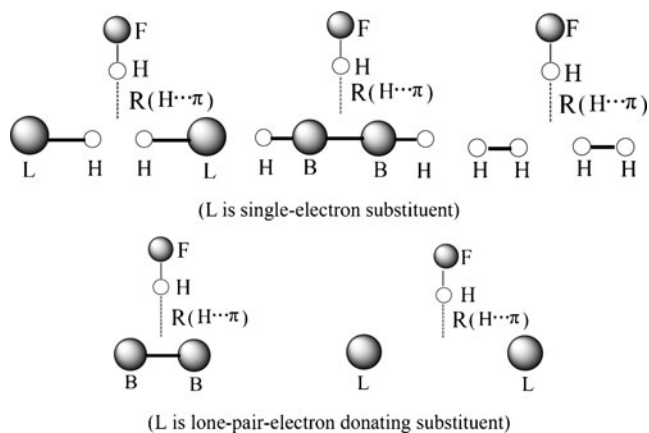
Fig. 2 The "truncated" model

respectively. It is up to −13.44 kJ mol^{-1} (43.20%) for NNB ≡ BNN…HF at B3LYP/6-311++G(2 d,p) level. For the complexes LBBL…HF (L = : CO, : NN, –CN and –NC), high percentage indicates the strong substituent effect on the T-shaped F–H…π interactions.

Analysis of the substituent effect using "truncated" model

To unravel the origin of the substituent effects in LBBL with single-electron substituent, a "truncated" model was constructed by replacing two boron atoms of the substituted LBBL (at the equilibrium separation of the corresponding complex) with the hydrogen atoms. The hydrogen was placed along the B–L bond, and the H–L distance was optimized with all other internal coordinates fixed. This similar model has been used to study substituent effects in the benzene dimer and the complex of substituted benzene C$_6$H$_5$X…Na$^+$ by Wheeler and Houk [36, 37]. Frontera et al. have reported through-space substituent effects in complexes of paracyclophanes with Na$^+$ and Li$^+$ [38]. We have

also used the "truncated" model to investigate the substituent effect on the cation-π interactions between Na$^+$ and LCCL [35].

In this work, the interaction energy of H$_2$ with H–F at a distance equal to R(H…π) for the corresponding LBBL… H–F complex is subtracted from the sum of $E_{int.(LH…F–H…HL)}$ and $E_{int.(F–H…HBBH)}$ to yield an additive approximation to the F–H…π binding energy [$E_{int.(LH…F–H…HL)}$ + $E_{int.(F–H…HBBH)}$ − $E_{int.(H2…F–H…H2)}$] (see Fig. 2). For the complexes with lone-pair-electron donating substituents, according to our method [35], interaction energies of F–H with substituted LBBL are captured by adding the L…F– H…L interaction to the F–H…BB interaction at a distance equal to R(F–H…π). Obviously, in two additive models, the effect of the substituent involves direct through-space interaction with the substituent.

From Table 3, for the single-electron substituents, the H…π interaction energy deviation −$E_{int.(LBBL…H–F)}$−[−($E_{int.(LH…H–F…HL)}$ + $E_{int.(H–F…HBBH)}$−$E_{int.(HH…H–F…HH)}$)] between the result for the intact substituted complex and the additive model is as follows: 14.74 kJ mol^{-1} (48.17%), 4.26 kJ mol^{-1} (40.49%) and 5.34 kJ mol^{-1} (36.20%) for the complexes with the substituents –Cl, –CN and –NC at (U) MP2(full)/6-311++G(2 d,p) level, respectively. High percentage indicates that the single-electron substituent effect plays an important role in the T-shaped F–H…π interaction. This is perhaps the reason why, although –Cl is the electron-withdrawing substituent, the T-shaped F–H…π interaction in ClBBCl…HF is stronger than that in HB = BH…HF. For the single-electron substituents, the additive model underestimates E_{int}.

For the lone-pair-electron substituents, the T-shaped X– H…π interaction energy deviations −$E_{int.(LBBL…H–F)}$−[−($E_{int.(L…H–F…L)}$ + $E_{int.(H–F…BB)}$)] are −16.58 kJ mol^{-1} (100.97%) and −8.64 kJ mol^{-1} (48.90%) for the complexes

Fig. 3 Shifts of electron density as a result of formation of the complex between HF and LBBL

HB=BH···HF   OCB≡BCO···HF   NNB≡BNN···HF

ClB=BCl···HF   NCB=BCN···HF   CNB=BNC···HF
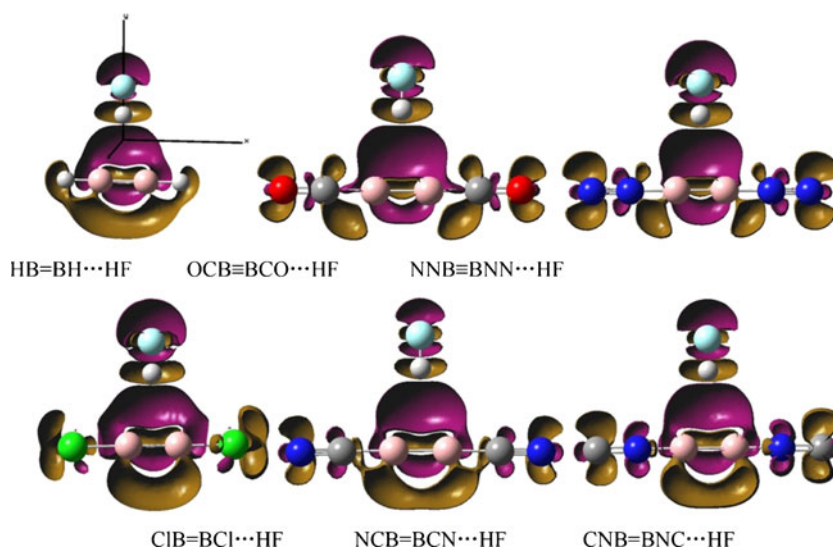
with : CO and : NN at (U)B3LYP/6-311++G(2 d,p) level, respectively. For these two complexes, the additive model overestimates E_{int}. In our previous investigation, for OCC ≡ CCO…Na$^+$, the additive model underestimates greatly E_{int} [35]. For OCB ≡ BCO…HF and NNB ≡ BNN…HF, the high percentages also indicate that the substituents : CO and : NN have a great influence on the T-shaped F–H…π interactions. This is perhaps the reason why, although both : CO and : NN are electron-donating substituents, the H…π interaction in OCBBCO…HF or NNBBNN… HF is weaker than that in HB = BH…HF.

Vibration frequencies

In order to obtain the information of the substituent effect on vibration frequencies, the frequency shifts are investigated. As can be seen from Table 4, for the complexes with LBBL (L = −H, : CO, –Cl, –CN and –NC), the frequencies of the stretching of the H…π bonds (ν_1) are predicted to be 150, 125, 225, 131 and 141 cm^{-1} at (U)MP2(full)/6-311++G(2 d,p) level. The values of the frequencies follow the order of ClBBCl…HF>HBBH… HF>CNBBNC…HF>NCBBCN…HF>OCBBCO…HF. In our recent investigation of substituent effect on the cation-π interaction between Na$^+$ and LCCL, the larger frequencies of the stretching of cation…π bonds are found in the complexes with the electron-donating substituents (in comparison with that in HCCH…Na$^+$) [35]. However, from Table 4, although –Cl is the electron-withdrawing substituent, the frequency of the stretching of the H…π bond in ClBBCl…HF is the largest. Except for OCBBCO…HF, the order of the frequency of the stretching of the H…π bond is well in agreement with that of the binding energy. In fact, a certain vibrational mode obtained from the calculation using Gaussian 03 programs is not one single vibrational frequency but a combination of several vibrational patterns. This is the reason why the order from the frequency of the H…π bond is not in accordance with that of the binding energy.

The larger the frequency shifts, the more stable the complex, so we also showed the important frequency shifts in order to investigate the relative stabilities of the complexes. The most important vibrational frequency of proton donor, ν_2, can be approximately described as the stretching of F–H. From Table 4, it can be seen that the ν_2 decreases (red shifts) and the IR intensity increases greatly in complexes in comparison with those in the monomer HF, showing the formation of the F–H…π interaction. The values of the frequency shifts follow the order of ClBBCl…HF >HBBH…HF>CNBBNC… HF >NCBBCN…HF >OCBBCO…HF at (U)MP2(full)/ 6-311++G(2 d,p) level. Except for OCBBCO…HF, it is consistent with the order of the binding energy.

In general, for the H…π hydrogen-bonded complex, due to electrons transfer from π-bond toward the hydrogen atom, the stretching of the π-bond will decrease (red shifts), and the multiple-bond will be weakened and elongated. Indeed, the symmetrical stretching frequencies of the BB bonds (ν_3) in LBBL…HF (L = −H, –NN and –Cl) decrease. However, the ν_3 increases in OCB ≡ BCO…HF (1537 cm^{-1}) in comparison with that in the monomer OCB ≡ BCO (1524 cm^{-1}) at (U)MP2(full)/6-311++G(2 d,p) level. This suggests that the B ≡ B bond in OCB ≡ BCO…HF might be contracted upon complexation, as is in accordance with the analysis of the structure above.

NBO analysis

The analyses of the structures, binding energies and "truncated" model have indicated that the substituents have great effect on the H…π interactions. To clarify further the nature of the substituent effects, the NBO analysis has been carried out.

According to the NBO analysis, all the T-shaped F–H…π hydrogen-bonded complexes have two units. The delocalization effects between them can be identified from the presence of off-diagonal elements of the Fock matrix in the NBO basis, and the strengths of these delocalization interactions, $E^{(2)}$ [28], can be estimated by second-order perturbation theory. From the results of $E^{(2)}$, we can see that the major T-shaped F–H…π interaction is that the BB bond offers the approximate sp$^{0.50}$ or p$^{1.00}$-hybridization π-electrons of the boron atoms to the contacting $\sigma_{(F–H)*}$ antibonding orbital.

From Table 5, the delocalization interaction $E^{(2)}\pi_{(BB)\rightarrow\sigma_{(HF)*}}$ in OCBBCO…HF is far weaker than that in HBBH…HF, and the value of the net charge transfer from LBBL to HF in OCBBCO…HF is also smaller than that in HBBH…HF. Therefore, the T-shaped F–H…π interaction in OCBBCO…HF is weaker than that in HBBH…HF. On the other hand, the stabilization energy $E^{(2)}\pi_{(LX)\rightarrow Lp(B)}$ is found in OCBBCO…HF (21.12 kJ mol^{-1}) and NNBBNN…HF (40.40 kJ mol^{-1}). This delocalization interaction shows that the : CO or : NN substituent does not offer the p$^{1.00}$-hybridization π-electrons to the contacting Lp(B)* antibonding orbital but to the Lp(B) bonding orbital. Thus, although the electron density in the BB bond is increased, the value of the net charge transfer from LBBL to HF in OCBBCO… HF or NNBBNN…HF does not increase. This result could be used to explain why, although both : CO and : NN are electron-donating substituents, the T-shaped F–H…π interactions in them are weaker than that in HB = BH… HF. The electron density accumulation of the B ≡ B bond (from : CO or : NN) leads to the contraction of the B ≡ B bond in OCBBCO…HF or NNBBNN…HF.

The notable p-π conjugation effect in ClBBCl…HF is confirmed. It originates mainly from the orbital interaction between the lone pair electrons of the Cl atom and π_{BB}* antibonding orbitals. $E^{(2)}_{Lp(Cl)\rightarrow\pi_{(BB)*}}$ has been predicted to be 105.85 kJ mol^{-1} at MP2(full)/6-311++G(2 d,p) level. High delocalization interaction leads to the high p-π conjugation effect, and consequently the electron density accumulation in the BB bond. The increased density tends to strengthen the T-shaped F–H…π interaction between ClBBCl and HF, as is in accordance with the result from binding energy.

For NCBBCN…HF and CNBBNC…HF, the π-π conjugation effects are obvious. The delocalization interactions $E^{(2)}_{\pi_{(BB)}\rightarrow\pi_{(LX)*}}$ are up to 115.93 and 85.90 kJ mol^{-1}, respectively. These delocalization interactions indicate that the BB bond offers the p$^{1.00}$-hybridization π-electrons of the boron atoms to the contacting $\pi_{(LX)*}$ antibonding orbital. The π-π conjugation effect decreases the charges on the boron atoms of the B = B double bond. Thus, the value of the net charge transfer from LBBL (L = −CN or −NC) to HF becomes smaller than that in HBBH…HF, and the delocalization interaction $E^{(2)}_{\pi_{(BB)}\rightarrow\sigma_{(HF)*}}$ in the former is also weaker than that in the latter. Therefore, the T-shaped F–H…π interaction in LBBL (L = −CN or −NC) is weaker than that in HBBH…HF.

AIM analysis

It is well known that the electronic characteristics are very essential to reveal the nature of the hydrogen bond. AIM method has been applied widely to study the hydrogen bonds of the complexes [22]. Our AIM results show that, for each F–H…π contact, there is a bond path linking the hydrogen atom with the midpoint of the BB bond, accompanied by a bond critical point (BCP) (see Fig. 1). The values of the electron densities $\rho_{BCP(H…\pi)}$ obtained are within a range of 0.0152 – 0.0250 au (see Table 1), and the corresponding Laplacians $\nabla^2\rho_{BCP(H…\pi)}$ are all positive, indicating the typical closed-shell kind of interactions and suggesting the formation of the T-shaped F–H…π interaction.

From Table 1, the value of the $\rho_{BCP(H…\pi)}$ in the complex with the lone-pair-electron donating substituent : CO is smaller than that in HB = BH…HF, indicating that the T-shaped F–H…π interaction in OCB ≡ BCO…HF is weaker than that in HB = BH…HF. The value of the $\rho_{BCP(H…\pi)}$ in the complex ClB = BCl…HF is larger than that in HB = BH…HF, showing a strong T-shaped F–H…π interaction between HF and ClB = BCl, as is consistent with the analysis of the binding energy. For the H…π hydrogen-bonded complex with the single-electron withdrawing substituent –CN or –NC, the value of the $\rho_{BCP(H…\pi)}$ is smaller than that in HB = BH…HF. This result shows that

the T-shaped F–H…π interaction in LB = BL…HF (L = −CN or –NC) is weaker than that in HB = BH…HF, as is in accordance with the result from the binding energy, too.

The change of the $\rho_{BCP(BB)}$ value upon complexation indirectly gives information of how the H…π interaction is affected by the substituent. As can be seen from Table 1, for the complexes with the single-electron substituents –Cl, –CN and –NC, the ρ_{BCP}(BB) values are smaller than those in the isolated monomers. However, for the complex with the lone-pair-electron substituent : CO, the ρ_{BCP}(BB) value is larger than that in the isolated monomer OCBBCO. This result shows that, for the complex OCB ≡ BCO…HF, the more lost density from the electron-donating substituent : CO in the complex than in the isolated monomer has been shifted to the π-bonding orbital of the BB bond upon complexation. This leads to the contraction of the B ≡ B bond upon complexation.

Analysis of the electron density shifts

In order to obtain deeper insight into the substituent effects on the T-shaped X–H…π interactions in detail, the analysis of the electron density shifts has also been carried out. The shifts of electron densities are illustrated in Fig. 3. These maps are generated by comparing the density in the complexes, point by point in space, to the same quantity in the isolated monomers. Purple regions represent the accumulation of additional electron density; yellow regions indicate loss of density.

The effects of the T-shaped H-bond formation are shown by the yellow region which is around the hydrogen atom of F–H bond, consistent with the accepted notion that the hydrogen loses density. The loss of the hydrogen atom density weakens the F–H bond, leading to this bond elongation and the decrease of strength. For the proton-accepting molecule, it is apparent by the notable yellow region around the BB bond axis that there is charge loss of the BB bond. Much of the charge loss is shifted toward the hydrogen atom of HF, indicated by the large purple upbow-region above the xz-plane including the BB bond, and little is shifted below the xz-plane (little purple area).

As can also be seen from Fig. 3, in the complexes LBBL…HF (: CO, : NN and –Cl), it is apparent by the purple region extending near to the BB bond axis that there is large charge buildup along the BB bond while the substituent moiety is surrounded by the notable yellow region, indicating that the substituent loses density. Many of these lost densities from the substituent moiety are shifted to the π-orbital of the BB bond upon complexation, leading to the electron density accumulation of the BB bond, as is consistent with the analyses of NBO and AIM. This is the origin of the effect p-π conjugation effect in

ClBBCl…HF and the contraction of the B ≡ B triple-bond in OCBBCO…HF and NNBBNN…HF.

For LBBL…HF (L = −CN and –NC), the notable purple region locates around the C ≡ N bond while the large yellow region is just below the BB bond, indicating that lost densities from the BB bond are partly shifted to the C ≡ N bond (partly toward HF). This indicates the single-electron withdrawing substituents effects for –CN and –NC (π-π conjugation).

Conclusions

The substituent effects on the intermolecular T-shaped F–H π interactions are investigated between HF and LBBL (L = −H, : CO, :NN, –Cl, –CN and –NC) using the (U)MP2(full) and (U)CCSD(T) methods with the 6-311++G(2 d,p) basis set. The B ≡ B triple bond contraction is found in the complexes with lone-pair-electron donors while the B = B double bond is lengthened in the systems with single-electron substituents upon complexation. The T-shaped F–H…π interaction energies follow the order of ClB = BCl…HF>HB = BH…HF>NNB ≡ BNN…HF>OCB ≡ BCO…HF>CNB = BNC…HF>NCB = BCN…HF. The electron-donating substituents : CO and :NN increase electron density of the B ≡ B triple bond by the delocalization interaction $E^{(2)}\pi_{(CO/NN)\rightarrow Lp(B)}$ while the electron-withdrawing substituents –CN and –NC decrease electron density of the B = B double bond by means of the π-π conjugative effect. The analyses of the APT atomic charge, "truncated" model, NBO, AIM and electron density shifts reveal the nature of the substituent effect and explain the origin of the B ≡ B bond contraction.

References

1. Meyer EA, Castellano RK, Diederich F (2003) Angew Chem Int Ed 42:1210–1250
2. Ehama R, Yokoo A, Tsushima M, Yuzuri T, Suezawa H, Hirota M (1993) Bull Chem Soc Jpn 66:814–818
3. Hirota M, Sakakibara K, Suezawa H, Yuzuri T, Ankai E, Nishio M (2000) J Phys Org Chem 13:620–623
4. Takahashi O, Kohno Y, Saito K (2003) Chem Phys Lett 378:509–515
5. Linares M, Pellegatti A, Roussel C (2004) J Mol Struct (THEOCHEM) 680:169–180
6. Vaupel S, Brutschy B, Tarakeshwar P, Kim KS (2006) J Am Chem Soc 128:5416–5426
7. Cornago P, Claramunt RM, Bouissane L, Elguero J (2008) Tetrahedron 64:3667–3673
8. Dauster I, Rice CA, Zielke P, Suhm MA (2008) Phys Chem Chem Phys 10:2827–2835
9. Karaminkov R, Chervenkov S, Neusser HJ (2008) Phys Chem Chem Phys 10:2852–2859
10. Knight LB Jr, Kerr K, Miller PK, Arrington CA (1995) J Phys Chem 99:16842–16848
11. Jouany C, Barthelat JC, Daudey JP (1987) Chem Phys Lett 136:52–56
12. Papakondylis A, Miliordos E, Mavridis A (2004) J Phys Chem A 108:4335–4340
13. Ren FD, Cao DL, Wang WL, Wang JL, Li YX, Hu ZY, Chen SS (2008) Chem Phys Lett 455:32–37
14. Perić M, Ostojić B, Engels B (1997) J Mol Spectrosc 182:295–308
15. Winther F, Schönhoff M, Huckauf A, Mkadmi EB (2002) J Mol Spectrosc 216:374–378
16. Gronowski M, Kołos R (2006) Chem Phys Lett 428:245–248
17. Gearhart DJ, Hunt KLC, Harrison JF (2008) J Mol Struct (THEOCHEM) 858:31–38
18. Gryff-Keller A (2002) J Mol Struct (THEOCHEM) 587:171–175
19. Jayakumar N, Kolandaivel P, Kuze N, Sakasumi T, Ohashi O (1999) J Mol Struct (THEOCHEM) 465:197–202
20. DiStasio RA, Helden GV, Steele RP, Head-Gordon M (2007) Chem Phys Lett 437:277–283
21. McDowell SAC (2004) J Mol Struct (THEOCHEM) 668:41–45
22. Ren FD, Cao DL, Wang WL, Ren J, Hou SQ, Chen SS (2009) J Mol Model 15:515–523
23. Ren FD, Cao DL, Wang WL, Ren J, Chen SS (2009) J Mol Struct (THEOCHEM) 896:38–43
24. Ren FD, Cao DL, Wang WL, Hou SQ, Chen SS (2008) J Mol Struct (THEOCHEM) 870:43–48
25. Cao DL, Ren FD, Liu SN, Chen SS (2009) J Mol Struct (THEOCHEM) 913:221–227
26. Xu WZ, Ren FD, Ren J, Liu SN, Yue Y, Wang WL, Chen SS (2010) J Mol Model 16:615–627
27. Frisch MJ, Trucks GA, Schlegel HB, Scuseria GE, Robb MA, Cheseman JR, Montgomery JA, Vreeven T, Kudin KN, Burant JC, Millam JM, Iyengar SS, Tomasi J, Barone V, Mennucci B, Cossi M, Scalmani G, Rega N, Petersson GA, Nakatsuji H, Hada M, Ehara M, Toyota K, Fukuda R, Hasegawa J, Ishida M, Nakajima T, Honda Y, Kitao O, Nakai H, Klene M, Li X, Knox JE, Hratchian HP, Cross JB, Adamo C, Jaramillo J, Gomperts R, Stratmann RE, Yazyev O, Austin AJ, Cammi R, Pomelli C, Ochtersky JW, Ayala PY, Morokuma K, Voth GA, Salvador P, Dannenberg JJ, Zakrzewski VG, Dapprich S, Daniels AD, Strain MC, Farkas O, Malick DK, Rabuck AD, Raghavachari K, Foresman JB, Ortiz JV, Cui Q, Baboul AG, Clifford S, Cioslowski J, Stefanov BB, Liu G, Liashenko A, Piskorz P, Komaromi L, Martin RL, Fox DJ, Keith T, Al-Laham MA, Peng CY, Nanayakkara A, Challacombe M, Gill PMW, Johnson B, Chen W, Wong MW, Gonzalez C, Pople JA (2003) Gaussian 03, Revision B.03. Gaussian Inc, Pittsburgh, PA
28. Reed AE, Curtis LA, Weinhold FA (1988) Chem Rev 88:899–926
29. Scheiner S, Kar T (2002) J Phys Chem A 106:1784–1789
30. Bader RFW (1990) Atoms in molecules-a quantum theory. Oxford University Press, Oxford, UK
31. Biegler-K nig FW, Bader RFW, Tang TH (1982) J Comput Chem 3:317–328
32. Duijineveldt FB (1994) Duijineveldt-van de Rijdt JCMV, Lenthe JHV. Chem Rev 94:1873–1885
33. Boys SF, Bernardi F (1970) Mol Phys 19:553–566
34. Tavares AM, da Silva WLV, Lopes KC, Ventura E, Araújo RCMU (2006) do Monte SA, da Silva JBP, Ramos MN. Spectrochim Acta A 64:412–417
35. Yang J, Ren F (2010) J Mol Struct (THEOCHEM) 956:1–9
36. Wheeler SE, Houk KN (2009) J Am Chem Soc 131:3126–3127
37. Wheeler SE, Houk KN (2009) J Chem Theor Comput 5:2301–2312
38. Frontera A, Quiñonero D, Garau C, Costa A, Ballester P, Deyà PM (2006) J Phys Chem A 110:5144–5148